Limnol. Oceanogr., 54(3), 2009, 666–680

Nitrate removal in stream ecosystems measured by ^{15}N addition experiments: Denitrification

Patrick J. Mulholland,[a,b,*] Robert O. Hall, Jr.,[c] Daniel J. Sobota,[d,1] Walter K. Dodds,[e] Stuart E. G. Findlay,[f] Nancy B. Grimm,[g] Stephen K. Hamilton,[h] William H. McDowell,[i] Jonathan M. O'Brien,[h] Jennifer L. Tank,[j] Linda R. Ashkenas,[d] Lee W. Cooper,[b,2] Clifford N. Dahm,[k] Stanley V. Gregory,[d] Sherri L. Johnson,[l] Judy L. Meyer,[m] Bruce J. Peterson,[n] Geoffrey C. Poole,[o,m] H. Maurice Valett,[p] Jackson R. Webster,[p] Clay P. Arango,[j,7] Jake J. Beaulieu,[j,3] Melody J. Bernot,[q] Amy J. Burgin,[h,4] Chelsea L. Crenshaw,[k,5] Ashley M. Helton,[m] Laura T. Johnson,[j] B. R. Niederlehner,[p] Jody D. Potter,[i] Richard W. Sheibley,[g,6] and Suzanne M. Thomas[n]

[a] Environmental Sciences Division, Oak Ridge National Laboratory, Oak Ridge, Tennessee
[b] Department of Ecology and Evolutionary Biology, University of Tennessee, Knoxville, Tennessee
[c] Department of Zoology and Physiology, University of Wyoming, Laramie, Wyoming
[d] Department of Fisheries and Wildlife, Oregon State University, Corvallis, Oregon
[e] Division of Biology, Kansas State University, Manhattan, Kansas
[f] Cary Institute of Ecosystem Studies, Millbrook, New York
[g] School of Life Sciences, Arizona State University, Tempe, Arizona
[h] Kellogg Biological Station, Michigan State University, Hickory Corners, Michigan
[i] Department of Natural Resources, University of New Hampshire, Durham, New Hampshire
[j] Department of Biological Sciences, University of Notre Dame, Notre Dame, Indiana
[k] Department of Biology, University of New Mexico, Albuquerque, New Mexico
[l] Pacific NW Research Station, U.S. Forest Service, Corvallis, Oregon
[m] Odum School of Ecology, University of Georgia, Athens, Georgia
[n] Ecosystems Center, Marine Biological Laboratory, Woods Hole, Massachusetts
[o] Department of Land Resources and Environmental Sciences, Montana State University, Bozeman, Montana
[p] Department of Biological Sciences, Virginia Polytechnic and State University, Blacksburg, Virginia
[q] Department of Biology, Ball State University, Muncie, Indiana

Abstract

We measured denitrification rates using a field ^{15}N–NO_3^- tracer-addition approach in a large, cross-site study of nitrate uptake in reference, agricultural, and suburban–urban streams. We measured denitrification rates in 49 of 72 streams studied. Uptake length due to denitrification (S_{Wden}) ranged from 89 m to 184 km (median of 9050 m) and there were no significant differences among regions or land-use categories, likely because of the wide range of conditions within each region and land use. N_2 production rates far exceeded N_2O production rates in all streams. The fraction of total NO_3^- removal from water due to denitrification ranged from 0.5% to 100% among streams (median of 16%), and was related to NH_4^+ concentration and ecosystem respiration rate (ER). Multivariate approaches showed that the most important factors controlling S_{Wden} were specific discharge (discharge / width) and NO_3^- concentration (positive effects), and ER and transient storage zones (negative effects). The relationship between areal denitrification rate (U_{den}) and NO_3^- concentration indicated a partial saturation effect. A power function with an exponent of 0.5 described this relationship better than a Michaelis–Menten equation. Although U_{den} increased with increasing NO_3^- concentration, the efficiency of NO_3^- removal from water via denitrification declined, resulting in a smaller proportion of streamwater NO_3^- load removed over a given length of stream. Regional differences in stream denitrification rates were small relative to the proximate factors of NO_3^- concentration and ecosystem respiration rate, and land use was an important but indirect control on denitrification in streams, primarily via its effect on NO_3^- concentration.

* Corresponding author: mulhollandpj@ornl.gov

Present addresses:
[1] School of Earth and Environmental Sciences, Washington State University, Vancouver Campus, Vancouver, Washington
[2] Chesapeake Biological Laboratory, University of Maryland Center for Environmental Science, Solomons, Maryland
[3] U.S. Environmental Protection Agency, Cincinnati, Ohio
[4] Cary Institute of Ecosystem Studies, Millbrook, New York
[5] Department of Biology, Utah State University, Logan, Utah
[6] USGS Washington Water Science Center, Tacoma, Washington
[7] Department of Geography, Central Washington University, Ellensburg, Washington

Humans have doubled inputs of fixed nitrogen (N) to the biosphere in recent decades (Vitousek et al. 1997; Galloway et al. 2004), causing increased hydrologic export of N from landscapes and consequent large increases in riverine inputs of N to estuaries and coastal oceans, primarily as nitrate–nitrogen (NO_3^-–N; Howarth et al. 1996; Jordan and Weller 1996). N loading to streams and rivers has accelerated rates of eutrophication and is implicated in development of extensive areas of anoxia and harmful algal blooms in a number of coastal ecosystems (Turner and Rabalais 1994; Glasgow and Burkholder 2000).

Regional budgets have shown that only about 10–25% of N added to land by humans is exported to the ocean (Howarth et al. 1996; Boyer et al. 2002; Schaefer and Alber 2007), indicating that substantial N sinks exist between land where N is applied and oceans receiving N loads. Streams and rivers may be important sinks for N owing to their high rates of biological activity and streambed sediment environments that favor microbial denitrification. In a study of the Mississippi River drainage basin, Alexander et al. (2000) showed that river networks were important sinks for dissolved N originating from terrestrial runoff. Peterson et al. (2001) developed a stream N-uptake model based on results from a cross-site ^{15}N addition study, and showed that biotic uptake could reduce inorganic N concentrations by about two-thirds over a 1-km stream reach.

A number of processes remove inorganic N from water, including assimilation by plants and microbes, sorption to sediments, deposition of particulate organic N, and denitrification. However, it is primarily denitrification that results in permanent loss while the other processes represent internal transformation or relocation. Rates of denitrification in streams and rivers have usually been estimated by mass-balance approaches or measured using the acetylene-block technique on sediment cores or slurries returned to the laboratory or in cores or chambers incubated in situ. Studies using the acetylene-block technique have generally shown that denitrification rates are highly variable in space and time, and are related primarily to redox status, NO_3^- concentration, and the availability of labile organic carbon (Duff et al. 1996; Holmes et al. 1996; Kemp and Dodds 2002). However, the acetylene-block technique is difficult to extrapolate to in situ rates because of handling of sediments if performed in the laboratory, modification of hydraulic conditions if conducted in field chambers, and inhibition of nitrification (Bernot et al. 2003). Thus, this technique may not provide accurate measures of denitrification rates for entire stream reaches, and may generate considerable uncertainty in extrapolating point estimates to larger scales.

Recently, several new approaches have been developed to measure denitrification at the scale of stream reaches. Mulholland et al. (2004) and Böhlke et al. (2004) describe a field ^{15}N–NO_3^- tracer-addition approach to quantify denitrification and total nitrate uptake rates. Laursen and Seitzinger (2002) and McCutchan et al. (2003) developed an approach using changes in N_2 concentrations over time or distance to estimate reach-scale denitrification rates. These reach-scale approaches provide the information needed to assess denitrification at the scale of entire river networks as demonstrated by Mulholland et al. (2008). An important issue for the response of streams to long-term increases in nitrogen loading is how denitrification rates will respond. It has been hypothesized that denitrification rates will saturate, but not as quickly as total uptake rates, because nitrate is being used in a dissimilatory process (electron acceptor for the oxidation of organic carbon) whereas assimilatory uptake will slow once it satisfies demands for growth (Bernot and Dodds 2005).

Here we report results of a large, cross-site study of denitrification using the reach-scale field ^{15}N–NO_3^- tracer-addition approach (second Lotic Intersite Nitrogen eXperiment [LINX II]). Experiments consisted of ^{15}N tracer additions to headwater streams across multiple biomes and land uses in the United States and Puerto Rico to provide in situ, reach-scale measurements of total NO_3^- uptake and denitrification. In a previous paper, we showed the strong effect of stream NO_3^- concentration on total uptake and denitrification rates across all biomes and land uses, and the implications of this relationship for NO_3^- removal in river networks (Mulholland et al. 2008). In a companion paper (Hall et al. 2009), we present a detailed analysis of total NO_3^- uptake and assimilatory uptake processes from the LINX II study, showing that NO_3^- concentration and gross primary production (GPP) rates are important controls. Here, we focus on denitrification as a mechanism for NO_3^- removal from stream water, and use multivariate techniques to show how hydrologic, geomorphic, and biologic factors interact to regulate denitrification rate. Our study addressed the following questions: (1) What are the most important proximate (direct) controls on denitrification rate and how do they interact to regulate denitrification uptake length and rate in streams across several biomes? (2) How does land use indirectly regulate denitrification through its effect on these proximate controls? (3) What is the best predictive model for denitrification uptake length and rate across a broad range of streams, including those with substantial anthropogenic influence? (4) Does denitrification rate become saturated with increasing NO_3^- concentration?

Methods

Study sites—We selected streams representing a wide range of biomes and land-use types. In each of eight regions (Fig. 1), we chose three headwater streams (generally first- or second-order, stream discharge <300 L s^{-1}) in each of three land-use categories (reference [i.e., the extant vegetation type for that biome], agricultural, suburban–urban), for a total of 72 streams (*see* Web Appendix: www.aslo.org/lo/toc/vol_54/issue_3/0666a.pdf). Streams were assigned to land-use categories based on visual observation of the dominant land use adjacent to the study reach. Reference streams were bordered by native vegetation according to biome and included forests, grassland, and desert shrub-land vegetation. Agricultural streams included a wide variety of cultivated lands, open-range grazing, and

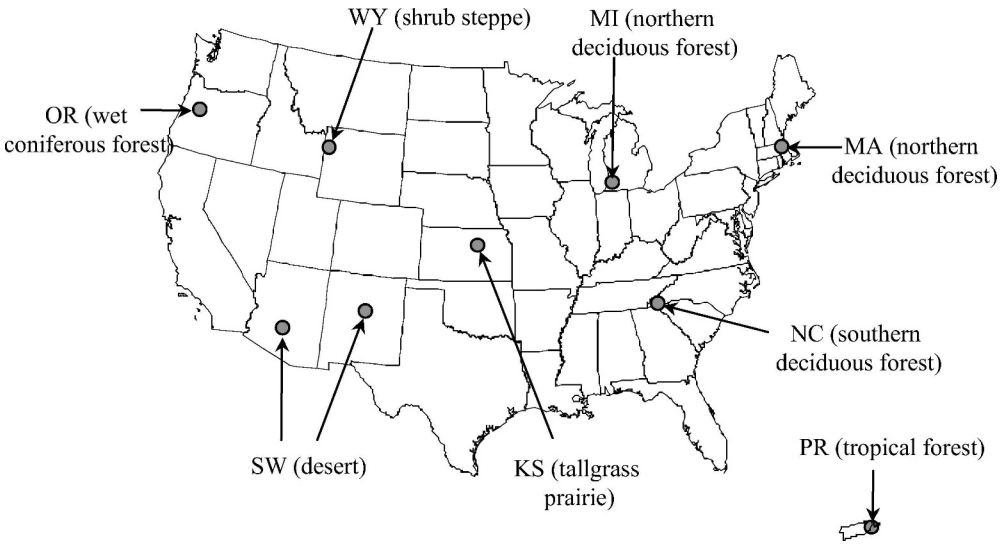

Fig. 1. Regional sites of LINX II study streams and the biomes represented. Abbreviations are Oregon (OR), Wyoming (WY), Michigan (MI), Massachusetts (MA), North Carolina (NC), Puerto Rico (PR), Kansas (KS), and Southwest (SW).

pastures. Suburban–urban streams included those bordered by housing developments, golf courses, and commercial areas, including a few with cement-lined channels. Selection of agricultural and suburban–urban streams was not necessarily intended to represent the dominant type of agricultural or suburban–urban environment but rather to provide a range of environments typical of each region. Many of the catchments drained by these streams had mixed land uses.

We determined land cover in the catchments of each stream using the United States Geological Survey (USGS) National Elevation Data Set (http://seamless.usgs.gov) and 2001 USGS National Land Cover Datasets (http://seamless.usgs.gov). For the Puerto Rico streams we used the 1991–1992 Landsat TM imagery as derived by Helmer et al. (2002). This a posteriori analysis of land cover at the catchment scale showed that reference streams drained catchments with >85% native vegetation (except for two streams with 50% and 65% native vegetation), whereas agricultural and suburban–urban streams drained catchments ranging from <1% to 100% agricultural and suburban–urban land-cover types.

^{15}N additions, sampling, and analysis—Experimental methods are outlined in a prior ^{15}N–NO_3^- addition study in Walker Branch, Tennessee (Mulholland et al. 2004) and in the online appendices to Mulholland et al. (2008) and described briefly here. We continuously added a $K^{15}NO_3$ (≥98% ^{15}N) and a conservative tracer (NaCl or NaBr) solution to each stream over a 24-h period using a peristaltic or fluid-metering pump. Isotope was added at rates designed to increase the $^{15}N:^{14}N$ ratio of streamwater NO_3^- ~20,000‰, which resulted in a relatively small (~7.5%) increase in the concentration of NO_3^- in stream water. We began isotope additions at ~13:00 h local time in each stream, completed additions at ~13:00 h the following day, and injected propane or SF_6 to measure air–water gas exchange rates within one day of the isotope-addition experiment.

Stream reaches of 105–1830 m (reach length was varied according to stream discharge and background NO_3^- concentration) were sampled at 6–10 locations downstream from the isotope-addition point. We measured ^{15}N flux in streamwater NO_3^-, N_2, and N_2O downstream from the addition point after downstream concentrations reached steady state. Samples for ^{15}N were collected once several hours prior to (to estimate natural-abundance ^{15}N levels) and two times after the isotope addition commenced: ~12 h (near midnight) and ~23 h (near noon). ^{15}N–NO_3^- was measured in filtered samples using a sequential reduction and diffusion method (Sigman et al. 1997). Samples were analyzed for ^{15}N on either a Finnigan Delta-S or a Europa 20–20 mass spectrometer in the Mass Spectrometer Laboratory of the Marine Biological Laboratory in Woods Hole, Massachusetts, a Europa Integra mass spectrometer in the Stable Isotope Laboratory of the University of California, Davis, or a ThermoFinnigan DeltaPlus mass spectrometer in the Stable Isotope Laboratory at Kansas State University.

Water samples for ^{15}N–N_2 and ^{15}N–N_2O were collected at each sampling location, equilibrated with He in 60- or 140-mL syringes, and injected into evacuated vials using underwater transfers of sample and gas to reduce the potential for air contamination (Hamilton and Ostrom 2007). Gas samples were analyzed for ^{15}N by mass spectrometry either using a Europa Hydra Model 20–20 mass spectrometer, a ThermoFinnigan DeltaPlus mass spectrometer, or a VG Instruments Prism Series II mass spectrometer (Biogeochemistry Laboratory, Department of Zoology, Michigan State University). ^{15}N content of all samples was reported in $\delta^{15}N$ notation where $\delta^{15}N = [(R_{SA}/R_{ST}) - 1] \times 1000$, and R is the $^{15}N:^{14}N$ ratio.

Results are expressed as parts per thousand (‰) deviation of the sample (SA) from the standard (ST), N_2 in the atmosphere ($\delta^{15}N = 0‰$). All $\delta^{15}N$ values were converted to mole fractions (MF) of ^{15}N [$^{15}N/(^{14}N + ^{15}N)$], and tracer ^{15}N fluxes (F) were calculated for each sample by multiplying the ^{15}N MF, corrected for natural abundances of ^{15}N by subtracting the average ambient ^{15}N MF for samples collected prior to the ^{15}N addition, by the concentrations of NO_3^-, N_2, or N_2O in stream water (C; concentrations of NO_3^- and N_2O were measured, whereas N_2 was taken as the concentration in equilibrium with air at the ambient stream temperature), and stream discharge (Q) derived from the measured conservative solute tracer concentrations ($F = MF \times C \times Q$).

NO_3^- uptake and denitrification rates—We measured rates of NO_3^- uptake for entire stream reaches based on the nutrient spiraling approach (Newbold et al. 1981; Stream Solute Workshop 1990). Total NO_3^- uptake was determined from the downstream rate of decline in tracer $^{15}NO_3^-$ mass flux using the model

$$d^{15}NO_3^-/dx = -k_{tot} \times {}^{15}NO_3^- \quad (1)$$

where $^{15}NO_3^-$ is the tracer $^{15}NO_3^-$ flux (μg ^{15}N s^{-1}), x is the stream channel distance from the tracer addition (m), and k_{tot} is the distance-specific NO_3^- uptake rate (m^{-1}).

Denitrification rates (calculated separately for production of N_2 and N_2O) were estimated by fitting a model of N gas production to the measured fluxes of tracer ^{15}N as N_2 and N_2O over the study reach as follows:

$$d^{15}NO_3^-/dx = -(k_{den} + k_U)^{15}NO_3^- \quad (2)$$

$$d^{15}N_{GAS}/dx = k_{den}{}^{15}NO_3^- - k_2{}^{15}N_{GAS} \quad (3)$$

where $^{15}NO_3^-$ is the tracer ^{15}N flux in NO_3^- (μg ^{15}N s^{-1}) and $^{15}N_{GAS}$ is the tracer ^{15}N flux in N_2 or N_2O (ng ^{15}N s^{-1}), k_{den} is the distance-specific N_2 or N_2O production rate (m^{-1}), k_U is the assimilative uptake rate of NO_3^- (m^{-1}), and k_2 is the air–water exchange of N_2 or N_2O. Values of k_2 for N_2 and N_2O were calculated from the measured rates of evasion of propane or SF_6 and the relative values of their Schmidt numbers (MacIntyre et al. 1995). Because the total uptake rate of NO_3^- (k_{tot}) is the sum of denitrification and assimilatory uptake (i.e., $k_{den} + k_U$), the equations above were solved only for k_{den} using the optimization tool "Solver" in Microsoft Office Excel (Mulholland et al. 2004).

Denitrification rates (k_{den}) were measured by model fitting only when there was significant tracer ^{15}N in N_2 or N_2O (defined as $\delta^{15}N$ values greater than the upper 97.5% confidence interval of background values measured prior to the isotope addition) at three or more stations along the stream reach. We then calculated the approximate 95% confidence interval for each k_{den} value using maximum likelihood estimates (MLE) assuming normally distributed errors (Hilborn and Mangel 1997) to assess whether k_{den} values were significantly >0 (i.e., 95% confidence interval of k_{den} did not include 0). We also applied MLE to ^{15}N-flux data from streams that did not meet the model-fitting criterion above (three stations with significant tracer ^{15}N in N_2 or N_2O) to determine if k_{den} was nonetheless sufficiently constrained to assign a nonzero value. Total k_{den} was then calculated as the sum of the k_{den} values for N_2 and N_2O. Uptake length of NO_3^- from denitrification (S_{Wden}, in m) is simply the inverse of total k_{den}.

Calculation of nutrient spiraling metrics—We calculated several additional denitrification rate metrics from k_{den} (Stream Solute Workshop 1990). Denitrification rate per unit time (k_{denT}, in d^{-1}) was calculated as

$$k_{denT} = k_{den} \times v \times 864 \quad (4)$$

where v is the average water velocity (cm s^{-1}) and 864 is a units-conversion factor. Denitrification uptake velocity (v_{fden}, in cm s^{-1}) was calculated as

$$v_{fden} = (Q/w) \times k_{den} \times 0.1 \quad (5)$$

where Q = discharge (L s^{-1}), w = average stream wetted width (m), and 0.1 is a units-conversion factor. Areal denitrification rate (U_{den}, in mg m^{-2} h^{-1}) was calculated as

$$U_{den} = (v_{fden} \times C) \times 3.6 \quad (6)$$

where C is the ambient NO_3^- concentration (μg N L^{-1}) and 3.6 is a conversion factor.

The denitrification fraction (fraction of total NO_3 uptake due to denitrification) was calculated as k_{den}/k_{tot}.

Measurements of other stream characteristics—Physical, chemical, and biological variables were measured in each stream within 3 d of the ^{15}N experiment to determine potential controls and predictors of denitrification rates. Average stream width (w) was calculated from measurements of wetted width at 5–10-m intervals along the experimental reach. Average discharge was measured by dilution of the conservative solute tracer. Average water velocity was measured by the time of travel of the rising limb of the conservative tracer profile and average depth was calculated as $Q/(w \times v)$. An advection–dispersion model with transient storage (OTIS-P; Bencala and Walters 1983; Runkel 1998) was applied to the conservative tracer data to determine hydraulic characteristics related to transient storage zones.

We collected water samples for chemical analysis at the same time and locations along the stream reach as the ^{15}N samples. Concentrations of NO_3^- were measured either by ion chromatography or by azo dye colorimetry after Cu–Cd reduction, NH_4^+ by phenate colorimetry or fluorometry, soluble reactive phosphorus (SRP) by ascorbic acid–molybdenum blue, and dissolved organic carbon by high-temperature combustion (Shimadzu TOC-V analyzer; American Public Health Association 1992).

Standing stocks of several benthic organic-matter components (coarse and fine benthic organic matter, epilithon, bryophytes, filamentous algae, vascular plants) were measured by collecting materials from a known area of the stream bottom at 5–10 locations within the study

reach. Dry mass (60°C) and ash-free dry mass (after combustion at 500°C) were determined on the material collected and extrapolated to the reach scale to estimate standing stocks.

Reach-scale rates of metabolism (GPP and ER) were measured using the diel dissolved-oxygen method (Odum 1956; Marzolf et al. 1994). Rates of air–water exchange of dissolved oxygen were calculated from the decline in dissolved propane or SF6 concentrations with distance (Marzolf et al. 1994) during gas injections conducted in conjunction with metabolism measurements.

Statistical analysis—To improve normality prior to parametric statistical analysis, all NO_3^- uptake parameters and other variables were $\log_{10}$-transformed, except denitrification fraction and catchment land-use fractions which were arcsine-square-root–transformed. Effect of region and land-use category were determined from two-way analysis of variance (ANOVA) and Dunnett's Multiple Comparison test with Bonferonni adjustment to determine significant differences among regions and land-use categories ($\alpha = 0.05$). Bivariate regressions were used to estimate relationships between the strongest individual predictors and denitrification rate. ANOVA and regression analysis were performed using SAS®, version 9.1 for Windows (SAS Institute).

We used two multivariate approaches to examine controls on S_{Wden} as described in Hall et al. (2009). The first was structural equation modeling (SEM) using observed variables (Shipley 2000; Grace 2006) to test a hypothesized pattern of causation with data based on a priori hypotheses as to the proximate controls of S_{Wden}. Using the package *sem* in R, we fit the expected covariance matrix based on the path model to the covariance matrix derived from the data by iteratively solving for a maximum likelihood solution (Fox 2006; R Development Core Team 2006). We used a chi-square–based goodness-of-fit test where $p > 0.05$ shows that the model structure is consistent with the data. We report unstandardized coefficients, rather than standardized coefficients, which allows measuring the direct effect of a predictor (e.g., NO_3^- concentration) on a response variable (Grace 2006). To estimate fraction of variation explained by the models, we calculated error variance for S_{Wden} in a model with standardized coefficients.

For the second approach, we evaluated a set of multiple linear regression (MLR) models to identify (1) what other variables besides those in the SEM analysis may serve as useful predictors of S_{Wden}, and (2) how the predictive capability of correlative MLR models compares with structured causal-based models of S_{Wden}. The set of MLR models were selected using Akaike's information criterion (AIC), which balances model predictive ability and parsimony (Akaike 1973). We applied a small sample size correction to AIC values (AIC_c) because of our relatively small sample size ($n = 44$; excluding missing values in explanatory terms; Burnham and Anderson 2002). We used a stepwise procedure to select a set of MLR models that predicted S_{Wden} with differences in AIC_c values (Δ_i) < 4.0 (Keeton et al. 2007). Explanatory variables that were available for model selection are presented in Table 1. Additionally, we calculated model likelihood (L), relative model likelihood (w_i), and multiple R^2 for each MLR model in candidate set (Burnham and Anderson 2002).

Results

We were able to calculate total NO_3^- uptake rates per unit stream length (k_{tot}) for 69 of the 72 streams studied (measurable rate of decline of tracer $^{15}NO_3^-$ with distance, *see* Hall et al. 2009), and were able to calculate total denitrification rates (k_{den}) for 49 of these streams (i.e., streams that met model-fitting criteria and for which the 95% confidence interval did not encompass 0 based on MLE analysis; *see* Web Appendix). All subsequent analyses and discussion are based on the results from these 49 streams.

N_2 production rates far exceeded N_2O production rates in all streams (results from two streams are shown in Fig. 2), with median N_2 production rate being 99.4% of the sum of N_2 and N_2O production rate (range = 94.3–99.9%). Because N_2O production was a small fraction of total denitrification rate, it will not be considered separately and our analyses hereafter are focused on total denitrification rate. Although insignificant as a component of denitrification, N_2O emissions contribute to atmospheric pools of this greenhouse gas, and LINX II data on in-stream production and emission rates of N_2O from the study streams will be the subject of another paper (J. Beaulieu unpubl.).

There were no consistent diurnal effects on denitrification rates. We could measure denitrification rate for both night and day samplings for 27 streams (i.e., both day and night $^{15}N_2$ data met the model-fitting criteria and MLE indicated that k_{den} was significantly >0, *see* Methods). Only 5 of the 27 streams had significantly higher denitrification rates at night than during the day and 2 of 27 had significantly higher denitrification rates during the day than at night (significance defined as nonoverlapping 95% CI). Of the 12 streams with relatively high rates of GPP (>1 g O_2 m^{-2} d^{-1}), only two had significantly higher denitrification rates at night than during the day. For all subsequent analyses, we averaged day and night denitrification rates for these streams.

S_{Wden} varied 2000-fold among streams, ranging from 89 m to 184 km (median of 9050 m), and there were no significant differences among regions or land-use categories (Fig. 3). In contrast, both region and land use contributed independently to the substantial variation in U_{den} among streams, which was from 0.004 mg N m^{-2} h^{-1} to 9.2 mg N m^{-2} h^{-1}, with a median of 0.58 mg N m^{-2} h^{-1} (Fig. 4). However, interaction between region and land use was not significant. Among regions, U_{den} was highest in Massachusetts and Michigan and lowest in Southwest streams (Fig. 4A). U_{den} also was about five times higher in suburban–urban streams than in reference streams (Fig. 4B).

Regional and land-use differences in U_{den} likely are the result of differences in NO_3^- concentration. ANOVA indicated that NO_3^- concentration was significantly higher in Michigan streams (mean of 570 μg N L^{-1}) and

Table 1. Best AIC_c models ($\Delta_i < 4.0$) predicting S_{Wden}. Sign of relationship is indicated for each variable in model. Variables that were available for model selection were: discharge, velocity, depth, stream gradient, water temperature, minimum daily dissolved oxygen concentration, NO_3^- concentration, NH_4^+ concentration, soluble reactive phosphorus concentration, dissolved organic carbon concentration, gross primary production rate (GPP), ecosystem respiration rate (ER), total detritus, fine benthic organic matter (FBOM), As : A ratio, F_{med}^{200}, and fraction of the catchment in agricultural, suburban–urban, and agricultural + suburban–urban land uses. All variables were log-transformed with the exception of land-use fractions which were arcsine-square-root–transformed.

Rank	Model covariates	AIC_c	Δ_i	Model likelihood	w_i*	R^2
1	+Velocity, +Depth, +NO_3^- concentration, −ER, −NH_4^+ concentration, −F_{med}^{200}	−62.98	0.00	1.00	0.32	0.64
2	+Velocity, +Depth, +NO_3^- concentration, −ER, −F_{med}^{200}	−62.29	0.68	0.71	0.22	0.60
3	+Velocity, +Depth, +NO_3^- concentration, −ER, −NH_4^+ concentration, −F_{med}^{200}, +Detritus	−61.29	1.68	0.43	0.14	0.65
4	+Velocity, +Depth, +NO_3^- concentration, −ER, −NH_4^+ concentration, −F_{med}^{200}, +Detritus, −FBOM, +As : A, −Gradient	−60.74	2.24	0.33	0.10	0.70
5	+Velocity, +Depth, +NO_3^- concentration, −ER, −NH_4^+ concentration	−60.48	2.50	0.29	0.09	0.59
6	+Velocity, +Depth, +NO_3^- concentration, −ER	−60.42	2.55	0.28	0.09	0.56
7	+Velocity, +Depth, +NO_3^- concentration, −ER, −NH_4^+ concentration, −F_{med}^{200}, −FBOM, +As : A, −Gradient, −GPP	−58.98	3.99	0.14	0.04	0.60

* w_i = Akaike weight.

significantly lower in Southwest streams (mean of 10 μg N L^{-1}), and was significantly higher in suburban–urban (mean of 298 μg N L^{-1}) compared to reference streams (mean of 47 μg N L^{-1}), suggesting that increasing NO_3^- concentrations stimulate U_{den}. We emphasize, however, that the effects of region shown here may not be indicative of regional differences in U_{den} because our streams were not selected as a random sample of streams in each region, particularly the agricultural and suburban–urban streams.

The fraction of total NO_3^- removal from water due to denitrification (denitrification fraction) ranged from 0.5% to 100% among streams, with a median of 15.8% (Fig. 5). Although denitrification fraction tended to be lower in the western streams (Kansas, Wyoming, Southwest, Oregon), differences among regions or land-use categories were not significant. Variation in denitrification fraction was related only to NH_4^+ concentration and ER (Fig. 6).

SEM identified relationships between potential controlling variables and S_{Wden}. Our hypothesized model of controls on denitrification was consistent with the data ($\chi^2 = 4.276$, df = 7, $p = 0.748$; Fig. 7A). In the simple model (Fig. 7A), which explained 64% of the variance in S_{Wden}, specific discharge (Q/w, which is equivalent to velocity × depth), NO_3^- concentration, ER, and F_{med}^{200} were significant direct controls, with increases in ER and F_{med}^{200} shortening S_{Wden} and increases in Q/w and NO_3^- increasing

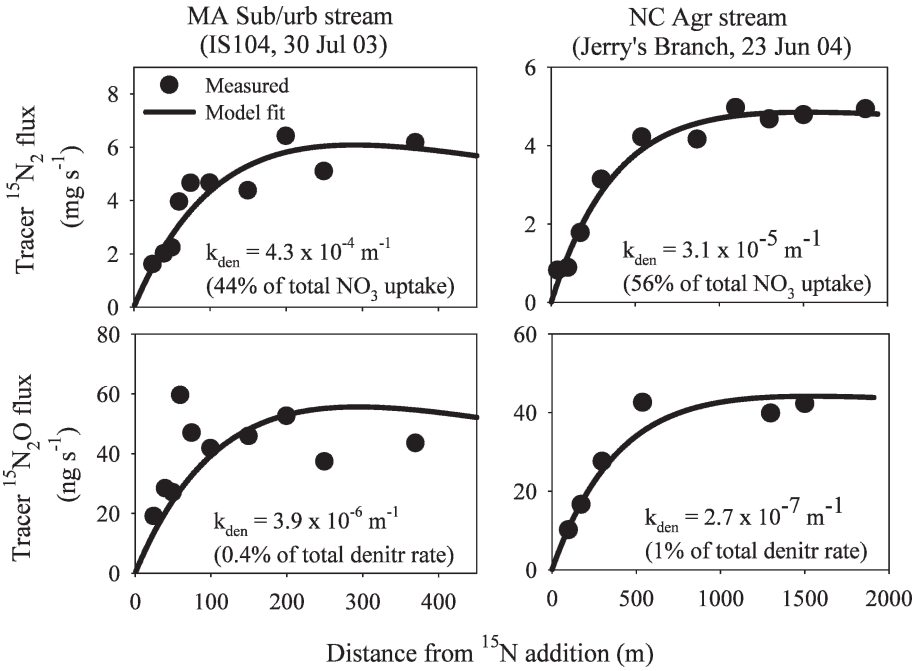

Fig. 2. Examples of best fits of the denitrification model to tracer $^{15}N_2$ and $^{15}N_2O$ flux data for two streams, a suburban–urban (Sub–urb) stream in Massachusetts (IS104) and an agricultural (Agr) stream in North Carolina (Jerry's Branch).

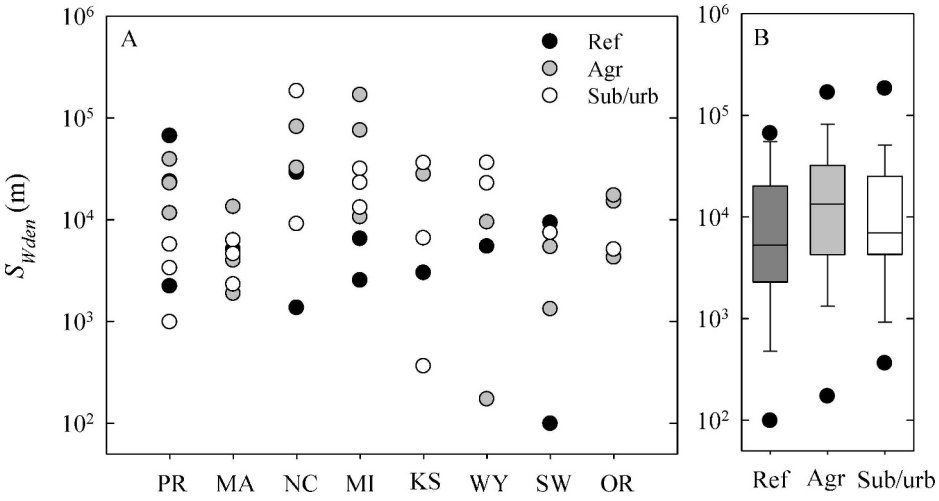

Fig. 3. Plot of denitrification uptake length (S_{Wden}) for (A) streams by region, and (B) box-and-whisker plot of S_{Wden} values by land-use category (plots display 10th, 25th, 50th, 75th, and 90th percentiles and individual data points outside the 10th and 90th percentiles). ANOVA indicated no significant effects of either region or land-use category.

S_{Wden}. F^{200}_{med} is a measure of the fraction of median water travel time due to transient storage within the stream reach and, thus, is a good measure of transient storage zone importance (Runkel 2002). Because S_{Wden} is the inverse of the fractional denitrification rate per unit stream length (k_{den}), these results indicate that k_{den} is stimulated by increasing ER and F^{200}_{med} but is reduced with increases in Q/w and NO_3^- concentration. Rate of GPP and NH_4^+ concentration were significant indirect controls on S_{Wden} via their influence on ER (autotrophic respiration or production of labile carbon via GPP, or both) and on NO_3^- concentration (nitrification), respectively. In addition to its direct effect, specific discharge (Q/w) indirectly affects S_{Wden} via its negative effect on F^{200}_{med}. We found a small (low path coefficient) but significant covariance between Q/w and ER which is unexplained.

The SEM path coefficients were derived using $\log_{10}$-transformed data and, thus, can be interpreted as scaling coefficients representing power–law relationships between S_{Wden} and different controlling factors (Fig. 7A). Comparison of path coefficients among the direct controls indicates that S_{Wden} was most sensitive to Q/w and least sensitive to F^{200}_{med}. Further, the path coefficient for Q/w was <1, indicating that the effect of Q/w on S_{Wden} was not proportional and that denitrification rate increased with increasing specific discharge.

Including land use measured as the fraction of watershed area in agriculture plus suburban–urban land use in the SEM also produced a model for S_{Wden} that was consistent with the data ($\chi^2 = 2.753$, df = 8, $p = 0.949$; Fig. 7B). We modeled land use as an indirect effect on S_{Wden} with significant positive effects on several proximate (i.e., direct) controlling factors. The fraction of human land use in the catchment increases concentrations of NH_4^+ and NO_3^-. Because both NO_3^- and NH_4^+ are increased by human land use and have opposite direct effects on S_{Wden}, the net indirect effect of land use on S_{Wden} is somewhat reduced. It is interesting that land use has a direct effect on GPP, but no direct effect on ER, the metabolism variable that does directly affect on S_{Wden}. It is also interesting that the significant linkage between NH_4^+ and NO_3^- concentrations in the simple model (Fig. 7A) disappears when land use is included (Fig. 7B), suggesting that the relationship between NH_4^+ and NO_3^- concentrations may be the result of covariance (i.e., both ions increase with land use) rather than a causal mechanism (nitrification).

Seven MLR models for S_{Wden}, selected according to AIC_c criteria, had sufficient evidence (ΔAIC_c values <4.0; Keeton et al. 2007) to be considered strong predictive models (Table 1). All of these models included water velocity, depth, NO_3^- concentration, and ER, indicating likely strong effects of these variables on S_{Wden}. In addition, NH_4^+ concentration and F^{200}_{med} were included in five of the seven models, also indicating effects on S_{Wden}. Several other stream characteristics were included in only one or two models, including total detritus and total fine benthic organic matter in the streambed, stream gradient, As : A ratio (a measure of the relative size of transient storage zones relative to the surface-water zone), and GPP. Therefore, we consider evidence for the importance of these variables weak. Land-use fraction was not included in any of the best predictive models, indicating that all land-use effects were captured in the other variables in these models. R^2 values for these models (ranging from 0.56 to 0.7) are similar to the R^2 of 0.64 for the path model (Fig. 7), suggesting that the latter includes the primary controls on S_{Wden}.

The relationship between U_{den} and NO_3^- concentration (Fig. 8A) was strong, in part because NO_3^- concentration was used in the computation of U_{den} from the measured parameters k_{den} and NO_3^- concentration (Eqs. 5 and 6). However, the best-fit power–law relationship ($\log U_{den} = -2.0 + 0.51 \log NO_3^-$; $R^2 = 0.37$) indicated a slope of 0.51 (95% CI of 0.32 to 0.70), significantly lower than the expected value of 1.0 based solely on the computation. This indicates a noncommensurate

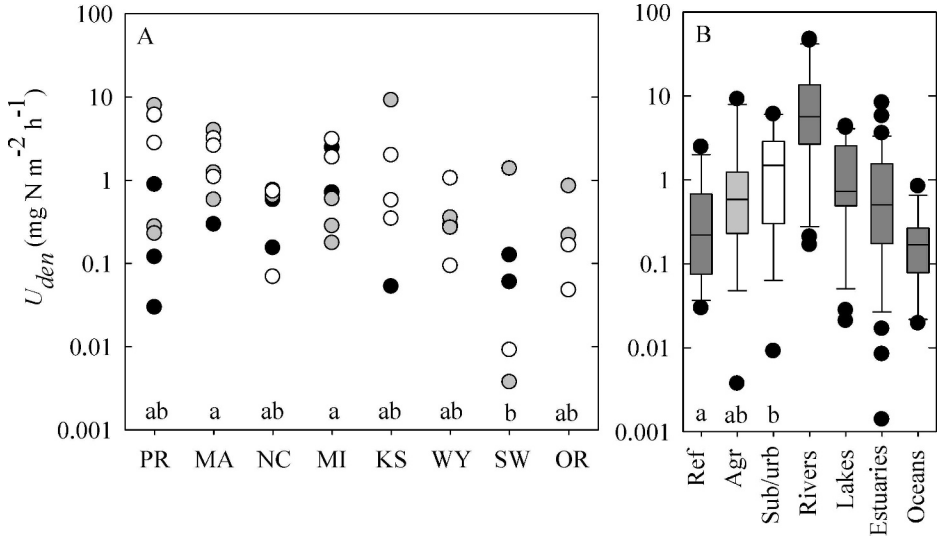

Fig. 4. Plot of areal denitrification rate (U_{den}) for (A) streams by region, and (B) box-and-whisker plot of U_{den} values by land-use category. Point or box shading denoting land-use category is the same as in Fig. 3. Lower case letters above region designations in panel A and land-use categories in panel B denote significant differences among groups determined by Dunnett Multiple Range test ($\alpha = 0.05$). Also shown in panel B are areal denitrification rates from a recent compilation of rates from other aquatic ecosystems by Piña-Ochoa and Álvarez-Cobelas 2006 (four dark shaded bars to right).

increase in U_{den} with increasing NO_3^- concentration (i.e., a saturating type of relationship). The best fit Michaelis–Menten relationship explained 26% of the variation in U_{den}, with a maximum U_{den} of 3.9 mg N m^{-2} h^{-1} and half-saturation NO_3^- concentration of 422 μg N L^{-1}. However, the Michaelis–Menten function did not fit the data as well as the power–law function (Fig. 8A). A few other reach-scale measurements of areal denitrification rate that have been reported in the literature are generally consistent with our U_{den} – NO_3^- concentration relationship (Fig. 8A). ER also was a significant predictor of U_{den} (Fig. 8B); however, it explained only 13% of the variation in U_{den}.

Discussion

Denitrification is one of the most challenging N-cycling processes to quantify, and yet it is thought to represent a substantial loss pathway for the massive increases in N deposited to terrestrial and aquatic ecosystems. Here, we show, using direct measurement of denitrification with a $^{15}NO_3^-$ tracer, that denitrification can account for a substantial fraction of the NO_3^- removal from streamwater in small streams of unaltered as well as agricultural and suburban–urban land uses. However, the large variation in denitrification rates and contribution to total NO_3^-

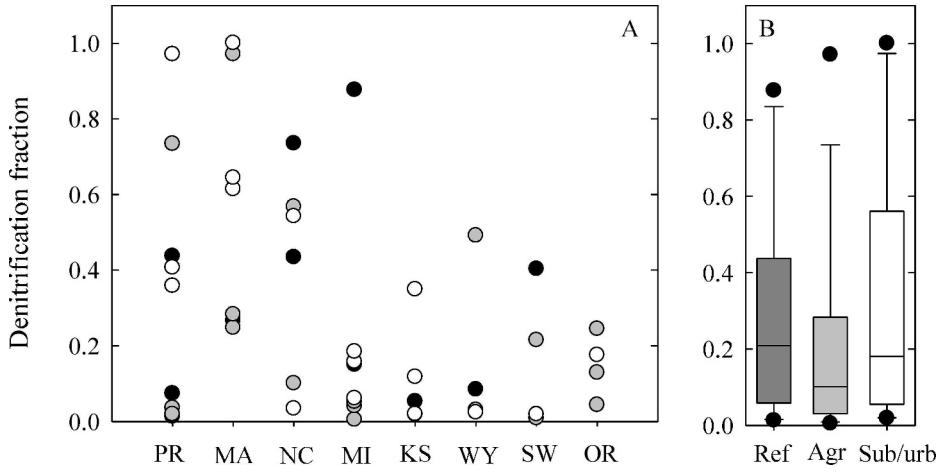

Fig. 5. Plot of denitrification fraction (fraction of total NO_3^- uptake rate) for (A) streams by region, and (B) box-and-whisker plot of denitrification fraction by land-use category. Point or box shading denoting land-use category is the same as in Fig. 3. ANOVA indicated no significant effects of either region or land-use category.

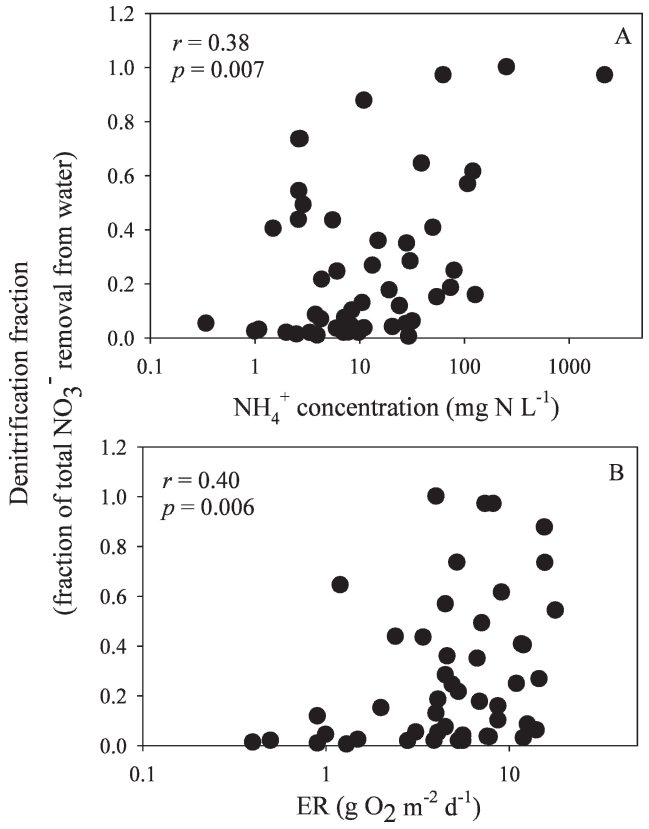

Fig. 6. Relationships between denitrification fraction and (A) NH_4^+ concentration and (B) ER. The *r*- and *p*-values listed are for correlations between arcsine-square-root–transformed denitrification fractions and log NH_4^+ or log ER.

removal that we observed across these diverse streams highlights the need for a mechanistic understanding of controls on this important process. Further, although this is the most comprehensive set of stream denitrification measurements to date, they represent a snapshot in time in each stream. Our data do not allow us to address the issues of seasonal or longer term variations in denitrification rate or its response to high flows.

Comparison with other measurements of denitrification rate—Across all regions and land uses, denitrification accounted for a median of ~16% of the total NO_3^- removal from stream water measured, with the remainder being assimilated by stream biota (Hall et al. 2009). This denitrification fraction is similar to that determined in an earlier tracer ^{15}N study in a small stream in the Southern Appalachian region of the U.S. with a low NO_3^- concentration (Mulholland et al. 2004), but is lower than the denitrification fraction of >0.5 estimated for a NO_3^--rich agricultural stream in the U.S. Midwest using a similar tracer ^{15}N approach (Böhlke et al. 2004). Although highly variable among our streams, the denitrification fraction was substantial for many streams, accounting for 40% or more of total NO_3^- removal from water in one-third of the streams. Because this is the first study to quantify this measure across a range of streams, we lack a basis for further comparison.

Based on our measurements of k_{den}, denitrification resulted in removal of 10% (median value, lower and upper quartile values of 4% and 22%, respectively) of streamwater NO_3^- over a 1-km reach of stream. By comparison, total uptake removed ~64% of streamwater NO_3^- over a 1-km reach in these streams (based on our measurements of k_{tot}). Using results from an earlier tracer ^{15}N study of N uptake in mostly pristine streams, Peterson et al. (2001) also reported that ~64% of the inorganic N inputs to streams could be removed over a 1-km stream reach by in-stream processes, although the importance of denitrification was not measured. Peterson et al. (2001) further showed that in-stream inorganic N removal was most sensitive to variations in NO_3^- removal relative to other N-cycling processes. Our results demonstrate that denitrification is an important mechanism for retention and removal of NO_3^- in streams across biomes and land uses, even though coupled denitrification is not accounted for with our method (*see* discussion below).

In a recent compilation of denitrification rates in aquatic ecosystems, Piña-Ochoa and Álvarez-Cobelas (2006) show that denitrification rates are considerably higher in rivers than in lakes, estuaries, and the ocean (Fig. 4B). Our denitrification rates are somewhat lower than those reported for rivers by Piña-Ochoa and Álvarez-Cobelas. Median U_{den} value for suburban–urban streams (1.5 mg N m^{-2} h^{-1}) is ~3.5 times lower than the median value for rivers reported by Piña-Ochoa and Álvarez-Cobelas, and the difference is even greater for agricultural and reference streams in our study. Some of the discrepancy may be due to differences in methods and spatial scale. Of the 24 denitrification rates reported by Piña-Ochoa and Álvarez-Cobelas for rivers, 13 were from studies using the acetylene inhibition technique and only four were reach-scale measurements using either ^{15}N or N_2 concentration methods, three of which were for systems with high NO_3^- concentration (>1 mg N L^{-1}).

Few published reach-scale stream denitrification rates are available. Two studies used tracer $^{15}NO_3^-$ additions (Böhlke et al. 2004; Mulholland et al. 2004) and two used changes in N_2 concentration to quantify stream reach-scale denitrification rates (Laursen and Seitzinger 2002; McCutchan et al. 2003). The latter studies were of streams that were considerably larger (discharges of 1.6–19 m^3 s^{-1}) than those in our study (<0.001–0.19 m^3 s^{-1}). The fact that these other reach-scale studies plot reasonably close to our U_{den}–NO_3^- relationship (Fig. 8A) suggests that our results are relatively robust, although more reach-scale measurements are needed, particularly in larger streams.

Measurement limitations—Denitrification rates we report here are likely underestimates of total denitrification in these streams because they include only denitrification of the extant pool of streamwater NO_3^-. Supply of NO_3^- for denitrification may also derive from the NO_3^- produced by nitrifiers in coupled mineralization–nitrification as has been shown for marine sediments (Laursen and Seitzinger 2001). Our measurements do not include this "coupled denitrification" if it is confined entirely to sediments and does not result in NO_3^- that exchanges with streamwater NO_3^- pools. Coupled denitrification may be the ultimate fate of a

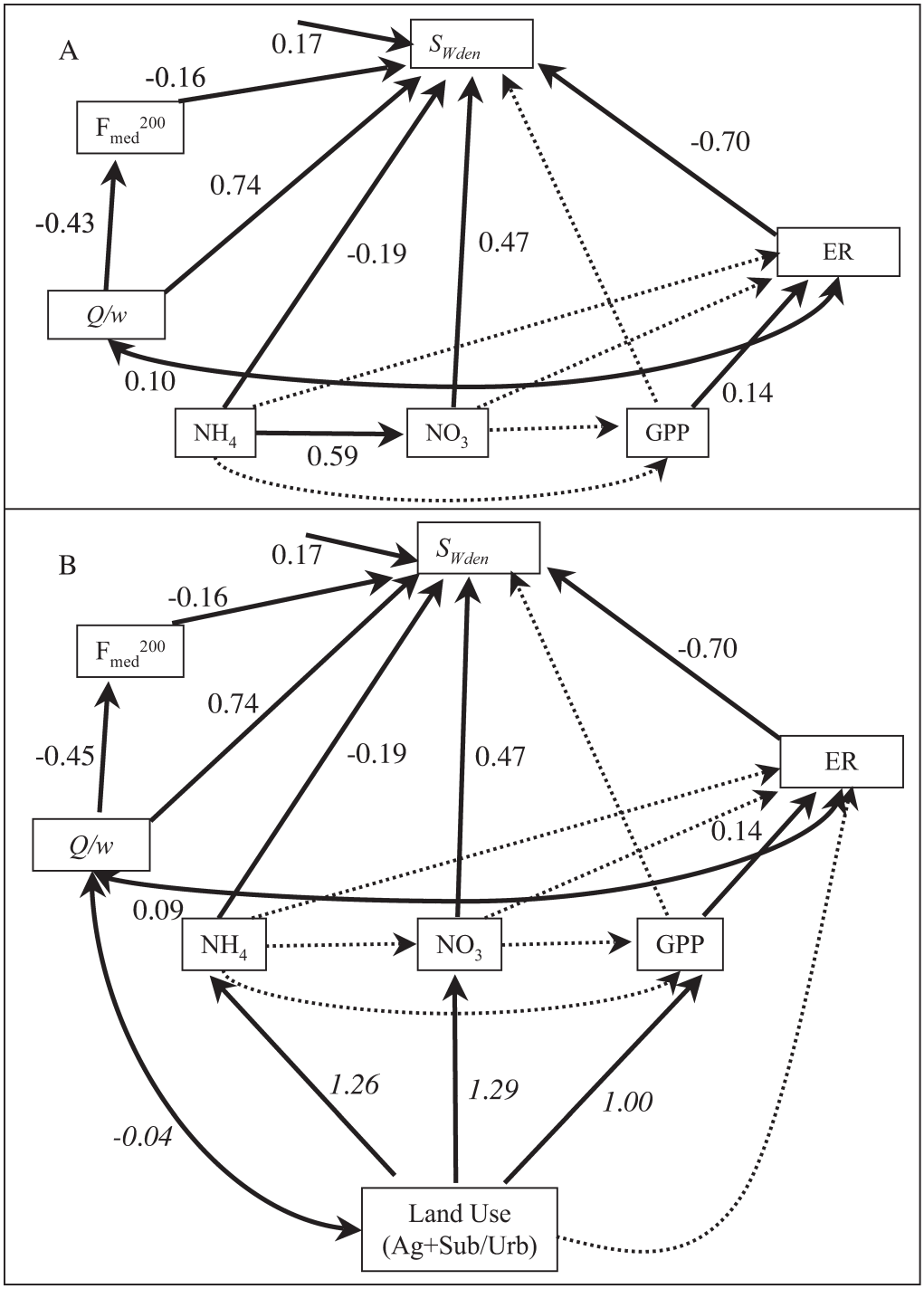

Fig. 7. Structural equation models describing controls of NO_3^- uptake length due to denitrification (S_{Wden}). Panel A presents the simple model ($\chi^2 = 4.276$, df = 7, $p = 0.748$), and panel B describes a more complex model that includes catchment land-use fraction ($\chi^2 = 2.753$, df = 8, $p = 0.949$). The catchment land-use fraction is the fraction of the catchment comprised by agriculture + suburban–urban land uses. Boxes are variables in the model and all variables were log-transformed except catchment land-use fraction, which was arcsine-square-root–transformed. Single-headed solid arrows are paths that are significantly different than 0 ($p < 0.05$) and dotted arrows are hypothesized paths that were found to be not significant. Double-headed arrows are unhypothesized covariances. Numbers are unstandardized path coefficients and can be interpreted as power–law coefficients, except for the italicized path coefficients leading from land use (panel B) because land use was arcsine-square-root–transformed. Error variance was calculated for all variables, and is shown for S_{Wden} (solid arrow not originating at a variable). Models in both panels A and B explained 64% of the variation in Log S_{Wden}.

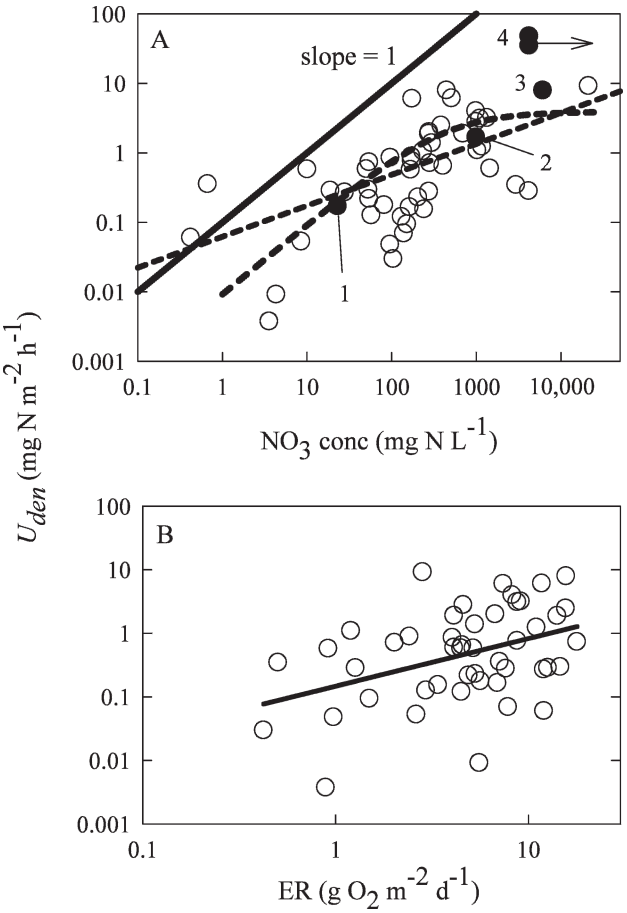

Fig. 8. Plot of U_{den} and (A) NO_3^- concentration and (B) ER. The numbered black data points in panel A are reach-scale denitrification rates determined using a similar $^{15}NO_3^-$ tracer approach (1 = East Fork Walker Branch, Mulholland et al. 2004; 2 = Sugar Creek, Illinois, Böhlke et al. 2004) or using a N_2 flux approach (3 = South Platte River, Colorado, McCutchan et al. 2003; 4 = Iroquois River, Illinois and Millstone River, New Jersey, Laursen and Seitzinger 2002). The NO_3^- concentrations for the Iroquois and Millstone Rivers were given only as >4200 μg N L^{-1} and the plotting uncertainty is indicated with the arrow. The solid line in panel A indicates a slope of 1 : 1, which is the expected slope based on the computation of U_{den} from measurements of k_{den} and NO_3^- concentration (Eqs. 5 and 6). The straight dashed line in panel A represents the power–law relationship (log U_{den} = −2.0 + 0.51 log NO_3^-; r^2 = 0.37). The curved dashed line represents the best fit Michaelis–Menten relationship (V_{max} = 3.9 mg N m^{-2} h^{-1}, K_m = 422 μg N L^{-1}, r^2 = 0.26). The solid line in panel B represents the power–law relationship (log U_{den} = −1.35 + 0.73 log ER; r^2 = 0.13).

portion of the assimilatory uptake of NO_3^- measured in our study (Hall et al. 2009). Coupled denitrification can be more important than denitrification of streamwater NO_3^- in aquatic ecosystems with NO_3^- concentrations <300 μg N L^{-1} (Seitzinger et al. 2006). Two-thirds (33 out of 49) of the streams in our study had NO_3^- concentrations <300 μg N L^{-1}; thus, total denitrification rates may be considerably higher than our measured rates in these streams.

Our ^{15}N experiments were conducted on one date in each stream, primarily during spring or summer months, and during periods of relatively low and stable flow in most streams. Thus, our measurements may not reflect mean annual denitrification rates in these streams. Our objective was to evaluate controls on denitrification across a broad variety of streams and conditions and not to assess variation in denitrification rates over time. A recent modeling study of denitrification in two river basins clearly showed the importance of seasonal variation in streamflow, with considerably lower removal of NO_3^- by denitrification during the higher flow spring period compared with lower flows in summer (Alexander et al. in press).

Controls on denitrification rate—Our results provide important new information on the physical, chemical, and biological factors that affect denitrification across a broad array of streams. Two statistical approaches (SEM and MLR) provided consistent evidence that a combination of hydrological (Q/w, equivalent to velocity × depth), chemical (NO_3^- and NH_4^+ concentrations), and biological (ER) factors were the most important controls of stream denitrification as quantified by S_{Wden}. In addition, both SEM and MLR indicated that transient storage zones (as quantified by F_{med}^{200}) influenced S_{Wden}, although not as strongly as other factors. Together these factors explain approximately two-thirds of the variation in S_{Wden}. Influence of the hydrological variables on S_{Wden} is expected because transport velocity and contact between water and the streambed where most biological activity occurs (inversely proportional to depth) are known to control uptake length of nutrients in streams (Newbold et al. 1981; Stream Solute Workshop 1990). However, the SEM coefficient for the Q/w–S_{Wden} path was 0.74, suggesting that S_{Wden} does not increase proportionately with an increase in specific discharge (a proportionate increase would result in a path coefficient of 1.0). This result was also observed for total uptake length of NO_3^- (Hall et al. 2009), and suggests that NO_3^- removal efficiency (v_{fden}, *see* discussion below) increases as stream size increases.

Effects of NO_3^- concentration and respiration—Analysis of S_{Wden} using SEM and MLR indicated that several factors other than hydrological properties also controlled denitrification across streams. NO_3^- concentration and ER exhibited the strongest effects, based on SEM path coefficients (Fig. 7) and inclusion of both of these variables in all MLR models (Table 1). Increasing NO_3^- concentration increased S_{Wden} indicating a reduction in the effectiveness of denitrification to remove NO_3^- from water as it flowed downstream, whereas increasing ER reduced S_{Wden}, indicating denitrification was more effective as a NO_3^- sink in streams with higher respiration rates. Analysis of denitrification expressed as an areal rate (U_{den}) also showed strong effects of NO_3^- concentration and ER based on univariate relationships.

Stronger evidence for the effect of NO_3^- concentration on denitrification is provided by relationships with denitrification uptake velocity (v_{fden}), a measure of the biological efficiency of denitrification relative to NO_3^- availability in stream water and one not computationally

influenced by NO_3^- concentration (Eq. 5). In a previous report of results from this study, we showed that v_{fden} was strongly related both to NO_3^- concentration and ER (Mulholland et al. 2008). The v_{fden}–NO_3^- relationship was a negative power–law function (slope of −0.49), indicating that higher NO_3^- concentration resulted in lower denitrification efficiency (lower v_{fden}). There was no effect of land-use category on the v_{fden}–NO_3^- relationship (interactive effect of land use and NO_3^- concentration was not significant; $p = 0.289$, SAS Proc GLM), indicating the primary effect of land use on v_{fden} was via effects on NO_3^- concentration. However, despite the loss of denitrification efficiency, areal denitrification rates increased with increasing NO_3^- concentration (Fig. 8A).

The significant effect of NH_4^+ concentration on both denitrification fraction (Fig. 6A) and S_{Wden} (Fig. 7) may be more evidence of the effect of NO_3^- availability on denitrification. When NH_4^+ concentrations are high, there may be a reduction in assimilatory demand for NO_3^- because NH_4^+ satisfies a greater proportion of the demand for inorganic fixed N for biosynthesis. As NH_4^+ becomes more available, denitrifiers may have increased access to NO_3^-, increasing the denitrification fraction as well as denitrification rate.

The strong, positive effect of ER on all measures of denitrification, including denitrification fraction (Fig. 6), may reflect wider distribution of zones of anoxia or hypoxia within the streambed of stream ecosystems because aerobic respiration decreases oxygen concentration. Although denitrification is an anaerobic process, it requires a supply of NO_3^- which can be supplied via nitrification, an aerobic process, and thus spatial heterogeneity in anaerobic and aerobic environments is important for high rates of denitrification. Such spatial heterogeneity may be enhanced in streambeds with high rates of aerobic respiration, thus enhancing denitrification. Further, denitrification is a facultative process and high rates of respiration suggest the presence of large populations of bacteria, which can potentially denitrify when conditions become favorable. ER may also be a surrogate measure for the availability of labile organic carbon required for dentrification, in the sense that both aerobic respiration (ER) and anaerobic respiration (i.e., denitrification) are controlled by available carbon substrates for decomposition. We did not find statistically significant relationships between denitrification rate parameters and several measures of organic matter abundance (dissolved organic carbon concentration, standing stocks of total detritus and fine benthic organic matter in the streambed); however, these latter measures may not adequately quantify labile organic carbon availability.

Comparison with other studies of denitrification controls—Our results showing the importance of NO_3^- concentration and ER as controls on denitrification are consistent with previous research, most of which was conducted in field chambers or in the laboratory. Many studies in streams and other aquatic ecosystems show that denitrification rates are controlled by NO_3^- concentration (García-Ruiz et al. 1998; Kana et al. 1998; Royer et al. 2004), by organic carbon availability (Caffrey et al. 1993; Holmes et al. 1996; Arango and Tank 2008), and by dissolved oxygen concentrations in the overlying water and in the upper layer of sediments (Christensen et al. 1990; Rysgaard et al. 1994). In addition, diurnal variations in denitrification can be related to photosynthetic oxygen production that reduces denitrification rates during the day (Christensen et al. 1990; Risgaard-Petersen et al. 1994). In contrast, Laursen and Seitzinger (2004) found higher denitrification rates during the day, which they attribute to elevated NO_3^- concentrations resulting from higher daytime nitrification rates under greater oxygen concentrations. Here, we found no consistent differences in denitrification rate between day and night.

In their meta-analysis of denitrification rates across aquatic ecosystems, Piña-Ochoa and Álvarez-Cobelas (2006) found significantly higher rates of denitrification (U_{den}) in ecosystems with high NO_3^- concentration (>700 μg N L^{-1}), high sediment interstitial dissolved organic carbon concentration (>10 mg g^{-1}), low dissolved oxygen concentration (<0.5 mg L^{-1}) and low total phosphorus concentration (<30 μg P L^{-1}). Multiple regression analysis, however, indicated that only NO_3^- and dissolved oxygen concentrations were significant predictors of denitrification rate, with NO_3^- concentration alone explaining 70% of the variability in denitrification rate (Piña-Ochoa and Álvarez-Cobelas 2006). Although we also found NO_3^- concentration to be the strongest single predictor for all denitrification metrics, stream dissolved oxygen concentration (either average or daily minimum values) did not relate to any denitrification measure with the exception of a positive relationship between minimum dissolved oxygen concentration and S_{Wden}. However, minimum dissolved oxygen concentration did not enter any of the MLR models (Table 1) and, therefore, the bivariate relationship may be spurious.

Denitrification–NO_3^- concentration relationship—Although many studies (including ours) have shown that areal denitrification rate (U_{den}) increases with increasing NO_3^- concentration, our study is the first to clearly demonstrate that the efficiency of denitrification declines with increasing NO_3^- concentration across multiple biomes. We measured denitrification efficiency (i.e., the fraction of NO_3^- available in water that is removed by denitrification) relative to both spatial (S_{Wden}) and temporal scales (v_{fden}). Here we show that the spatial efficiency of denitrification declined (S_{Wden} increases) with increasing NO_3^- concentration (Fig. 7). As noted above, Mulholland et al. (2008) showed that the temporal efficiency of denitrification (v_{fden}) also declined with increasing NO_3^- concentration. Further, Mulholland et al. (2008) showed that the decline in denitrification efficiency with increasing NO_3^- concentration can have important implications for NO_3^- removal in stream networks and its response to anthropogenic NO_3^- loading to streams, with larger streams becoming more important in NO_3^- removal within the network as loading rates increase and smaller streams become saturated with nitrogen.

Saturation of N cycling rates is an important issue that has been well-studied in terrestrial systems, but poorly understood in streams (Bernot and Dodds 2005). Prior

research has suggested three potential models for areal denitrification rates (U_{den}): (1) no saturation (first-order model), (2) a Michaelis–Menten type saturation (Seitzinger 1988), and (3) an efficiency loss model described by a power–law function with an exponent of <1.0 (O'Brien et al. 2007). Our results suggest that the efficiency loss model is more appropriate when considering denitrification rates across a wide variety of streams (Fig. 8A). Although a Michaelis–Menten model may be appropriate for describing the denitrification–NO_3^- concentration relationship in a particular stream under a particular set of biological conditions (e.g., constant microbial population), our data suggest that this form of saturation kinetics is not the best model for denitrification rates across streams. A power–law function appears to be the better model probably because denitrification involves multiple mechanisms and controls across the wide range of stream conditions and NO_3^- concentrations reflected in this study.

Effects of transient storage zones—Our results are consistent with other studies indicating that transient storage zones (including hyporheic zones) are important sites for denitrification in streams (Duff and Triska 1990; Triska et al. 1993). Denitrification rates were greater (S_{Wden} shorter) in streams with longer water residence time in transient storage zones, as indicated by higher F_{med}^{200}. However, F_{med}^{200} did not appear to exert as strong an effect on S_{Wden} as other controls, because the absolute value of its path coefficient in SEM was considerably lower than those for the other significant direct controls of S_{Wden} (Fig. 7) and it was not included in all MLR models (Table 1). Our measurements of transient storage zones include both hyporheic (within benthic sediments) and in-channel backwater zones, and the latter may not be a primary site of denitrification in streams. The effect of transient storage zones on denitrification may require further study distinguishing these two types of storage zones and flow paths. In their recent review, Seitzinger et al. (2006) have suggested that denitrification is controlled by the interactions between geomorphology and hydrology that establish flow paths and water residence times. This is likely to be particularly true for streams.

Effects of land use—Our experimental design allowed us to assess the effects of land use across multiple biomes. Land-use category had no direct effect on S_{Wden} and denitrification fraction (Figs. 3 and 5), and catchment land-use fraction was not significantly related to these parameters and did not enter as a significant predictor in the MLR models for S_{Wden}. Instead, the effect of land use on denitrification was indirect, primarily via effects on NH_4^+ and NO_3^- concentrations. Increasing proportion of agriculture and suburban–urban land use within the catchment resulted in higher concentrations of NO_3^- and NH_4^+, as well as higher rates of GPP (Fig. 7B). Increases in NH_4^+ concentrations led to increases in the spatial efficiency of denitrification (shorter S_{Wden}; Fig. 7B) and greater denitrification fraction (Fig. 6A), whereas increases in NO_3^- concentration resulted in increases in areal denitrification rates (Fig. 8A), but decreases in the spatial efficiency of denitrification (S_{Wden}; Fig. 7B). Increases in GPP had little effect on denitrification, although increases in GPP had a large positive effect on total uptake rates of NO_3^- (Hall et al. 2009). Although the effect of land use was indirect, it was nonetheless important given the strength of its effect on NO_3^- and NH_4^+ concentrations, as indicated by the high coefficients for these paths in Fig. 7B.

Here we show that NO_3^- concentration is the key to understanding and predicting denitrification rates in streams. Although areal rates of denitrification (U_{den}) increase with increasing NO_3^- concentration, the efficiency of NO_3^- removal from water via denitrification declines, resulting in a smaller proportion of streamwater NO_3^- load being removed as water flows over a given length of stream (k_{den}, or $1/S_{Wden}$). Our results suggest that regional differences in denitrification are small relative to the proximate factors of NO_3^- concentration and ecosystem respiration rate. Land use is an important but indirect control on denitrification in streams, primarily via its effect on NO_3^- concentration. This result is important because it indicates that land use per se may not be critical, but rather the NO_3^- loading to streams from land uses that increase that loading is the important factor.

The permanent removal of nitrogen via denitrification is an ecosystem service provided by streams. If a stream management objective is to achieve high efficiency of NO_3^- removal via denitrification to ensure the health of downstream ecosystems, lower NO_3^- loadings that maintain concentrations at <1 mg N L^{-1} are required. Many streams in agricultural and suburban–urban settings exceed these values and, therefore, already contribute to downstream ecosystem degradation. Improvement in N removal efficiency in these streams will require reduction in NO_3^- loading. Our results clearly show that reduction in NO_3^- loading as well as maintaining biological integrity and the capacity to retain organic matter that fuels respiration are crucial ingredients for efficient removal of NO_3^- via denitrification in streams. Future studies should address the issues of seasonal or longer term variations in denitrification rate or its response to high flows that we were unable to address in this study.

Acknowledgments

This work was supported by National Science Foundation (NSF) grant DEB-0111410 to the University of Tennessee, NSF Long Term Ecological Research (LTER) grants to some of the individual sites, and numerous smaller grants and fellowships to other institutions. More than 100 students and scientists gathered the information for this synthesis paper. We thank Nathaniel Ostrom for assistance with stable isotope measurements of N_2 and N_2O and Wil Wollheim for initial development of the model that we modified to estimate denitrification rates from field data. We thank Charles Garten and two anonymous reviewers for comments that improved earlier versions of the manuscript. We also thank the NSF LTER network, U.S. Forest Service, National Park Service and many private landowners for permission to conduct experiments on their lands. Partial support to PJM during manuscript preparation was provided by the U.S. Department of Energy, Office of Science, Biological and Environmental Research under contract DE-AC05-00OR22725 with UT-Battelle LLC.

References

AKAIKE, H. 1973. Information theory as an extension of the maximum likelihood principle, p. 267–281. *In* B. N. Petrov and F. Csaki [eds.], Second international symposium on information theory. Akademiai Kiado.

ALEXANDER, R. B., AND OTHERS. In press. Hydrological and biogeochemical effects on stream denitrification and nitrogen loads in river networks. Biogeochemistry.

———, R. A. SMITH, AND G. E. SCHWARZ. 2000. Effect of stream channel size on the delivery of nitrogen to the Gulf of Mexico. Nature **403:** 758–761.

AMERICAN PUBLIC HEALTH ASSOCIATION. 1992. Standard methods for the examination of water and wastewater. American Public Health Assoc.

ARANGO, C. P., AND J. L. TANK. 2008. Land use influences the spatiotemporal controls on denitrification in headwater streams. J. North Am. Benthol. Soc. **27:** 90–107.

BENCALA, K. E., AND R. A. WALTERS. 1983. Simulation of solute transport in a mountain pool-and-riffle stream: A transient storage model. Water Resour. Res. **19:** 718–724.

BERNOT, M. J., AND W. K. DODDS. 2005. Nitrogen retention, removal, and saturation in lotic ecosystems. Ecosystems **8:** 442–453.

———, ———, W. S. GARDNER, M. J. MCCARTHY, D. SOBOLEV, AND J. L. TANK. 2003. Comparing denitrification estimates for a Texas estuary by using acetylene inhibition and membrane inlet mass spectrometry. Appl. Environ. Microbiol. **69:** 5950–5956.

BÖHLKE, J. K., J. W. HARVEY, AND M. A. VOYTEK. 2004. Reach-scale isotope tracer experiment to quantify denitrification and related processes in a nitrate-rich stream, mid-continent USA. Limnol. Oceanogr. **49:** 821–838.

BOYER, E. W., C. L. GOODALE, N. A. JAWORSKI, AND R. W. HOWARTH. 2002. Anthropogenic nitrogen sources and relationships to riverine nitrogen export in the northeastern U.S.A. Biogeochemistry **57/58:** 137–169.

BURNHAM, K. P., AND D. R. ANDERSON. 2002. Model selection and multimodel inference: A practical information-theoretic approach, 2nd ed. Springer.

CAFFREY, J. M., N. P. SLOTH, H. F. KASPAR, AND T. H. BLACKBURN. 1993. Effect of organic loading on nitrification and denitrification in a marine sediment microcosm. FEMS Microbiol. Ecol. **12:** 159–167.

CHRISTENSEN, P. B., L. P. NIELSEN, J. SØRENSEN, AND N. P. REVSBECH. 1990. Denitrification in nitrate-rich streams: Diurnal and seasonal variation related to benthic oxygen metabolism. Limnol. Oceanogr. **35:** 640–651.

DUFF, J. H., C. M. PRINGLE, AND F. J. TRISKA. 1996. Nitrate reduction in sediments of lowland tropical streams draining swamp forest in Costa Rica: An ecosystem perspective. Biogeochemistry **33:** 179–196.

———, AND F. J. TRISKA. 1990. Denitrification in sediments from the hyporheic zone adjacent to a small forested stream. Can. J. Fish. Aquat. Sci. **47:** 1140–1147.

FOX, J. 2006. Structural equation modeling with the sem package in R. Struct. Eq. Model. **13:** 465–486.

GALLOWAY, J. N., AND OTHERS. 2004. Nitrogen cycles: Past, present, and future. Biogeochemistry **70:** 153–226.

GARCÍA-RUIZ, R., S. N. PATTINSON, AND B. A. WHITTON. 1998. Denitrification in river sediments: Relationship between process rate and properties of water and sediment. Freshw. Biol. **39:** 467–476.

GLASGOW, H. B., AND J. M. BURKHOLDER. 2000. Water quality trends and management implications from a five-year study of a eutrophic estuary. Ecol. Appl. **10:** 1024–1046.

GRACE, J. B. 2006. Structural equation modeling in natural systems. Cambridge Univ. Press.

HALL, JR., R. O., AND OTHERS. 2009. Nitrate removal in stream ecosystems measured by ^{15}N addition experiments: Total uptake. Limnol. Oceanogr. **54:** 653–665.

HAMILTON, S. K., AND N. E. OSTROM. 2007. Measurement of the stable isotope ratio of dissolved N_2 in ^{15}N tracer experiments. Limnol. Oceanogr. Methods **5:** 233–240.

HELMER, E. H., O. RAMOS, T. D. M. LOPEZ, M. QUINONES, AND W. DIAZ. 2002. Mapping the forest type and land cover or Puerto Rico, a component of the Caribbean Biodiversity Hotspot. Caribb. J. Sci. **38:** 165–183.

HILBORN, R., AND M. MANGEL. 1997. The ecological detective: Confronting models with data. Princeton Univ. Press.

HOLMES, R. M., J. B. JONES, JR., S. G. FISHER, AND N. B. GRIMM. 1996. Denitrification in a nitrogen-limited stream ecosystem. Biogeochemistry **33:** 125–146.

HOWARTH, R. W., AND OTHERS. 1996. Regional nitrogen budgets and riverine N and P fluxes for the drainages to the North Atlantic Ocean: Natural and human influences. Biogeochemistry **35:** 75–139.

JORDAN, T. E., AND D. E. WELLER. 1996. Human contributions to terrestrial nitrogen flux. BioScience **46:** 655–664.

KANA, T. M., M. B. SULLIVAN, J. C. CORNWELL, AND K. M. GROXZKOWSKI. 1998. Denitrification in estuarine sediments determined by membrane inlet mass spectrometry. Limnol. Oceanogr. **43:** 334–339.

KEETON, W. S., C. E. KRAFT, AND D. R. WARREN. 2007. Mature and old-growth riparian forests: Structure, dynamics, and effects on Adirondack stream habitats. Ecology **17:** 852–868.

KEMP, M. J., AND W. K. DODDS. 2002. The influence of ammonium, nitrate, and dissolved oxygen concentrations on uptake, nitrification, and denitrification rates associated with prairie stream substrata. Limnol. Oceanogr. **47:** 1380–1393.

LAURSEN, A. E., AND S. P. SEITZINGER. 2001. The role of denitrification in nitrogen removal and carbon mineralization in Mid-Atlantic Bight sediments. Cont. Shelf Res. **22:** 1397–1416.

———, AND ———. 2002. Measurement of denitrification in rivers: An integrated whole reach approach. Hydrobiologia **485:** 67–81.

———, AND ———. 2004. Diurnal patterns of denitrification, oxygen consumption and nitrous oxide production in rivers measured at the whole-reach scale. Freshw. Biol. **49:** 1448–1458.

MACINTYRE, S., R. WANNINKHOF, AND J. P. CHANTON. 1995. Trace gas exchange across the air–water interface in freshwater and coastal marine environments, p. 52–97. *In* P. A. Matson and R. C. Harriss [eds.], Biogenic trace gases: Measuring emissions from soil and water. Methods in ecology. Blackwell.

MARZOLF, E. R., P. J. MULHOLLAND, AND A. D. STEINMAN. 1994. Improvements to the diurnal upstream–downstream dissolved oxygen change technique for determining whole-stream metabolism in small streams. Can. J. Fish. Aquat. Sci. **51:** 1591–1599.

MCCUTCHAN, JR., J. H., J. F. SAUNDERS III, A. L. PRIBYL, AND W. M. LEWIS, JR. 2003. Open-channel estimation of denitrification. Limnol. Oceanogr. Methods **1:** 74–81.

MULHOLLAND, P. J., AND OTHERS. 2008. Stream denitrification across biomes and its response to anthropogenic nitrate loading. Nature **452:** 202–205.

———, H. M. VALETT, J. R. WEBSTER, S. A. THOMAS, L. N. COOPER, S. K. HAMILTON, AND B. J. PETERSON. 2004. Stream denitrification and total nitrate uptake rates measured using a field ^{15}N isotope tracer approach. Limnol. Oceanogr. **49:** 809–820.

Newbold, J. D., J. W. Elwood, R. V. O'Neill, and W. Van Winkle. 1981. Measuring nutrient spiraling in streams. Can. J. Fish. Aquat. Sci. **38:** 860–863.

O'Brien, J. M., W. K. Dodds, K. C. Wilson, J. N. Murdock, and J. Eichmiller. 2007. The saturation of N cycling in Central Plains streams: ^{15}N experiments across a broad gradient of nitrate concentrations. Biogeochemistry **84:** 31–49.

Odum, H. T. 1956. Primary production in flowing waters. Limnol. Oceanogr. **1:** 102–117.

Peterson, B. J., and others. 2001. Control of nitrogen export from watersheds by headwater streams. Science **292:** 86–90.

Piña-Ochoa, E., and M. Álvarez-Cobelas. 2006. Denitrification in aquatic environments: A cross-system analysis. Biogeochemistry **81:** 111–130.

R Development Core Team. 2006. R: A language and environment for statistical computing. R Foundation for Statistical Computing, Vienna, Austria. ISBN 3-900051-07-0. Available from: http://www.R-project.org.

Risgaard-Petersen, N., S. Rysgaard, L. P. Nielsen, and N. P. Revsbech. 1994. Diurnal variation of denitrification in sediments colonized by benthic microphytes. Limnol. Oceanogr. **39:** 573–579.

Royer, T. V., J. L. Tank, and M. B. David. 2004. Transport and fate of nitrate in headwater agricultural streams in Illinois. J. Environ. Qual. **33:** 1296–1304.

Runkel, R. L. 1998. One-dimensional transport with inflow and storage (OTIS): A solute transport model for streams and rivers. U.S. Geological Survey, Water Resources Investigation Report 98-4018.

———. 2002. A new metric for determining the importance of transient storage. J. North Am. Benthol. Soc. **21:** 529–543.

Rysgaard, S., N. Rysgaard-Petersen, N. P. Sloth, K. Jensen, and L. P. Nielsen. 1994. Oxygen regulation of nitrification and denitrification in sediments. Limnol. Oceanogr. **39:** 1643–1652.

Schaefer, S. C., and M. Alber. 2007. Temperature controls a latitudinal gradient in the proportion of watershed nitrogen exported to coastal ecosystems. Biogeochemistry **85:** 333–346.

Seitzinger, S. P. 1988. Denitrification in freshwater and coastal marine ecosystems: Ecological and geochemical significance. Limnol. Oceanogr. **33:** 702–724.

———, and others. 2006. Denitrification across landscapes and waterscapes: A synthesis. Ecol. Appl. **16:** 2064–2090.

Shipley, B. 2000. Cause and correlation in biology. Cambridge Univ. Press.

Sigman, D. M., M. A. Altabet, R. Michener, D. C. McCorkle, B. Fry, and R. M. Holmes. 1997. Natural abundance-level measurement of the nitrogen isotopic composition of oceanic nitrate: An adaptation of the ammonia diffusion method. Mar. Chem. **57:** 227–242.

Stream Solute Workshop. 1990. Concepts and methods for assessing solute dynamics in stream ecosystems. J. North Am. Benthol. Soc. **9:** 95–119.

Triska, F. J., J. H. Duff, and R. J. Avanzino. 1993. Patterns of hydrological exchange and nutrient transformation in the hyporheic zone of a gravel-bottom stream: Examining terrestrial–aquatic linkages. Freshw. Biol. **29:** 259–274.

Turner, R. E., and N. N. Rabalais. 1994. Coastal eutrophication near the Mississippi river delta. Nature **368:** 619–621.

Vitousek, P. M., and others. 1997. Human alteration of the global nitrogen cycle: Sources and consequences. Ecol. Appl. **7:** 737–750.

Associate editor: Samantha B. Joye

Received: 15 April 2008
Accepted: 29 September 2008
Amended: 02 November 2008